THE EFFECT OF NEUTRALISATION METHOD AND REAGENT ON THE RATE OF CU AND ZN RELEASE FROM ACID ROCK DRAINAGE TREATMENT SLUDGES[1]

Danny M. McDonald[2], John A. Webb[2], Robert J. Musgrave[2]

Abstract. Neutralisation of Acid Rock Drainage (ARD) by adding an alkaline reagent produces sludges generally dominated by amorphous ferrihydrite, often with high levels of adsorbed heavy metals. The effect of neutralisation method and reagent on the long-term chemical stability of these treatment sludges was investigated experimentally using a relatively oxidised synthetic ARD (containing Fe[~70% Fe^{+3}], Al, Cu and Zn) with a variety of reagents and processes, and two reduced synthetic ARD compositions (Fe^{+2}, Al, Cu and Zn; Fe^{+2}, Cu and Zn) treated with hydrated lime. The sludges were all subjected to kinetic testing to determine the rate of Cu and Zn release at pH 4, simulating disposal in a moderately acidic pit lake. All sludges precipitated from the oxidised ARD by standard ARD neutralisation procedures and reagents (lime, limestone, Bauxsol, KB-1 and HDS lime) showed similar chemical stability, with an initial rapid rate of release of Cu and Zn (~50% of leaching in the first 5 minutes) that reduced over time, apparently exponentially. The Cu and Zn are adsorbed onto the surface of the amorphous ferrihydrite present.

Sludges initially precipitated as ferrous hydroxide and then oxidised may contain a finely crystalline goethite component; if the ARD was Al-free the crystalline content is greater and coarser-grained and may consist of magnetite as well as goethite. Leaching of zinc from these crystalline sludges can be as much as an order of magnitude less than from sludges precipitated as ferric hydroxide, due to the incorporation of Zn within the mineral structure. Copper is more readily released from the sludges with a higher goethite/magnetite content, because it is adsorbed on the crystallite surfaces. However, it appears that Al-rich goethite can incorporate Cu, reducing its leachability.

Thus, modifications to the ARD treatment procedure, in particular control of oxidation state and Al levels, can substantially increase the crystallinity and improve the chemical stability of the sludge precipitated, and have a much greater influence on sludge leachability than the neutralisation agent used. These modifications are probably applicable to any water treatment sludges formed by pH adjustment.

Additional Key Words: ARD, neutralisation, sludge, leaching, magnetite, goethite, crystallinity, KB-1, Bauxsol

Introduction

Neutralization of Acid Rock Drainage (ARD) by adding an alkaline reagent, usually hydrated lime, produces sludges generally dominated by poorly crystalline/amorphous $Fe(OH)_3$ (ferrihydrite), often with high levels of adsorbed heavy metals, and frequently also containing gypsum. The long-term chemical stability of these ARD treatment sludges is a significant problem, because they have the potential to release metals back into the environment if they are exposed to low pH water. As a result ARD treatment sludges may be classified as hazardous waste, limiting disposal options; disposal can often represent a significant proportion of overall ARD treatment costs.

The most widely used tests to assess the leachability of ARD treatment sludges have been the Toxicity Characteristic Leaching Procedure (TCLP, US EPA method 1311), designed to simulate co-disposal with municipal (putrescible) waste, and the Synthetic Precipitation Leaching Procedure (SPLP, US EPA method 1312), which simulates an acid rain scenario. Neither of these procedures was specifically designed for evaluating ARD treatment sludge leachability, and as a result they do not model the low pH of common mine site disposal environments. McDonald *et al.* (in press), developed a new leach test (Strong Acid Leach Test, SALT) that more closely reflects mine disposal environments where sludges could come in contact with a virtually unlimited supply of acid, lowering the pH of the sludge pore water. SALT involves a series of leach tests with increasing strengths of H_2SO_4 extractant solution added to each test, so that the most acid leachate solution has a pH of <2.5 after 18 hours of end over end mixing. The proportion of metals leached was plotted against pH to derive a leaching curve for the sludge being tested.

SALT testing of the common neutralisation processes (Batch neutralisation, High Density Sludge) and neutralisation reagents (lime, limestone and the proprietary reagents KB-1 and Bauxsol) showed that the resistance of ARD treatment sludges to leaching by low pH waters is not affected by the reagent or process used for treatment (McDonald *et al.* in press), despite some claims to the contrary. None of the reagents investigated provided significantly different results from the other reagents, other than Bauxsol and KB-1, which leached more Al (these reagents contain Al). As expected, the lower the pH of the leaching solution, the more metals that were leached from the sludge. Iron, Al, Cu, and Zn began to be leached at pH values of 3, 4.5, 5.5 and 6.5, respectively. A sludge's chemical stability was found to depend on its neutralising potential, which is usually the amount of lime or limestone within the sludge, and in general reflects the treatment (reagent use) efficiency.

In order to better understand how and why heavy metals are leached from ARD treatment sludges, two new approaches were used. Firstly, the rate of metal release was investigated, using a kinetic leaching test, in which the pH is maintained at 4 and samples are taken periodically for 18 hours. The kinetic test simulates disposal of ARD treatment sludge in a moderately acidic environment, such as a pit lake or ARD collection pond, and can by itself provide a good indication of the chemical stability of the sludge, although SALT results are required to fully characterise sludge leachability.

Secondly, the conditions of ARD neutralisation were varied so that reduced ferrous hydroxide precipitates were produced and then oxidised to $Fe(OH)_3$; the chemical stability of these treatment sludges was assessed using the kinetic leach test and compared with the leachability of $Fe(OH)_3$ sludges prepared following standard neutralisation techniques. This

procedure was used because mine site neutralisation of ARD has often been noted to produce a sludge that is initially greenish, indicating a $Fe(OH)_2$ component, and then oxidises to the brown colour typical of $Fe(OH)_3$ (e.g. at Brukunga in South Australia; Earth Systems 2004). Ferric iron is more chemically stable than Fe^{+2} iron (e.g. Stumm and Morgan 1996), and $Fe(OH)_3$ precipitates are more resistant to acid leaching than Fe^{+2} (Watzalf and Casson 1990). For this reason many ARD treatment plants include an oxidation (air sparging) step to ensure that the sludge precipitated contains only Fe^{+3} iron. In the present experiments the $Fe(OH)_2$ sludge initially precipitated was oxidised to $Fe(OH)_3$ prior to leach testing, in order to determine the long-term leachability of the sludge in its most chemically stable form.

Methods

Preparation of synthetic ARD

Three ARD compositions were used in experiments; all contained relatively high levels of acidity and metals to maximise the mass of sludge generated, whilst still replicating likely field ARD compositions.

The first synthetic ARD contained 1200 mg/L Fe (~70% Fe^{3+}), 110 mg/L Al, 100 mg/L Cu and 100 mg/L Zn (all ± 10 mg/L), added as metal SO_4^{-2} salts to tap water, as used in experiments described by McDonald *et al.* The pH was lowered to 2.3 with H_2SO_4, giving a total SO_4^{-2} concentration of approximately 4000 mg/L. The ARD was a dark translucent brown colour due to the predominance of Fe^{+3} iron.

To test the influence of change in oxidation state of iron during sludge precipitation, it was decided to run a series of experiments that initially precipitated a $Fe(OH)_2$ sludge, which would then be oxidised. To ensure $Fe(OH)_2$ precipitation, all the Fe in the ARD used was in the reduced Fe^{+2} oxidation state. Otherwise the second ARD composition was virtually the same as the first; the Fe concentration was slightly higher (1400 mg/L Fe), and the pH was not decreased with H_2SO_4, giving a slightly higher pH of 3.5. The higher pH meant that less hydrated lime was needed to neutralise the acidity, and as a result less gypsum was precipitated in the neutralisation sludge. The tap water used to make the ARD was sparged with N_2 gas for 30 minutes to remove O_2, prior to adding the metal salts. The ARD was a light translucent green color due to the presence of Fe^{+2} iron.

The third ARD composition was identical to the second composition, except that it did not contain Al. This synthetic ARD was used for a single experiment to assess the effect of Al on the mineralogy of treatment sludge, as Al is believed to have an inhibitory effect on the crystal growth of Fe oxides and hydroxides (Cornell and Schwertmann 2003).

Neutralisation of ARD

The synthetic ARD was neutralised using four procedures (Table 1): a 170L batch reactor, a 15L batch reactor, a laboratory scale High Density Sludge (HDS) plant with sludge recycle, and a lab scale batch analogue of a HDS plant. Both batch and HDS neutralisation methods are widely used within the mining industry, (e.g. Aube and Zinck 1999, Brown *et al.* 2002, Kuyucak *et al.* 2005, Lewis *et al.* 2003, Portefield *et al.* 2003).

The large batch reactor was used for Runs 1–6, which were designed to test the chemical stability of sludges precipitated using oxidised ARD (dominantly Fe^{+3} iron) and different neutralisation reagents (Table 1). It was a 170 L polyethylene tank in which 150 L batches of

Table 1. Details of neutralisation process (Runs 1-7 after McDonald *et al.* in press)

Run Name	Neutralisation Equipment	ARD composition	Neutralisation Reagent	Final Treatment pH	pH of supernatant water after settling (24h)	Reagent Use	Reaction Time (minutes)[1]	Air Sparging
Run 1	170 L reactor	ferric	15 wt% hydrated lime slurry	10.04	9.19	4.06 g/L	189	Started 95 minutes after neutralisation started
Run 2	170 L reactor	ferric	15 wt% hydrated lime slurry	9.57	8.85	3.64 g/L	64	Continuous
Run 3	170 L reactor	ferric	15 wt% limestone slurry 15 wt% hydrated lime slurry	5.17 9.55	 9.09	5.85 g/L 4.99 g/L	53 92	Continuous
Run 4	170 L reactor	ferric	15 wt% limestone slurry 15 wt% hydrated lime slurry	5.17 9.11	7.71 (after 4 days sparging) 8.85	5.88 g/L 0.26 g/L	77 5	Continuous, including for four days between adding $CaCO_3$ and $Ca(OH)_2$
Run 5	170 L reactor	ferric	15 wt% KB-1 slurry	9.41	9.18	5.07 g/L	152	Continuous
Run 6	170 L reactor	ferric	Bauxsol powder, added directly to ARD at the Virotech recommended rate of 0.3g/L/4 hours.	8.22	8.33	11.71 g/L	21 days	No sparging as neutralisation was conducted over 21 days.
Run 7	HDS Plant. 250L of ARD was treated to allow time for density to build up.	ferric	10 wt% hydrated lime slurry. Lower concentration slurry used to reduce chance of HDS plant blockage.	Reagent added as required to keep reactor 2 at a pH of 9.	8.37	3.46 g/L	133 min (water) / 26.7 hr (sludge)[2]	Continuous into all 3 reactors

[1] Reaction time for Runs 1–6, 8–11 is the time taken to add reagent. Further reagent dissolution or Fe oxidation may occur after this.

[2] Average residence time of water/sludge in HDS plant after initial start-up period. Total treatment time for Run 7 was 8 days.

Run Name	Neutralisation Equipment	ARD composition	Neutralisation Reagent	Final Treatment pH	pH of supernatant water after settling (24h)	Reagent Use	Reaction Time (minutes)[1]	Air Sparging
Run 8	15 L reactor	ferrous	10 wt% hydrated lime slurry	10.25	9.50	N/A	14	Started after neutralisation finished
Run 9	15 L reactor	ferrous	10 wt% hydrated lime slurry	10.24	9.50	N/A	15	Started after neutralisation finished
Run 10	15 L reactor	ferrous	10 wt% hydrated lime slurry	9.77	9.50	N/A	126	Continuous, H_2O_2 also added as oxidant
Run 11	15 L reactor	ferrous	10 wt% hydrated lime slurry	9.58	9.50	N/A	445	Continuous, H_2O_2 also added as oxidant
Run 12a	Batch HDS system	ferrous, without Al	10 wt% hydrated lime slurry	~9, slightly different for each cycle	Did not drop as iron was not oxidised	N/A	6 days	Started after neutralisation finished
Run 12b	Batch HDS system	ferrous, without Al	10 wt% hydrated lime slurry	~9, slightly different for each cycle	Did not drop as iron was not oxidised	N/A	6 days	Started after neutralisation finished

Table 2. Dominant mineralogy of ARD treatment sludges as determined by XRD; for minor phases in Runs 1-7 sludges, see McDonald et al. (in press). See Table 1 for detail on run conditions.

	Run 1	Run 2	Run 3	Run 4	Run 5	Run 6	Run 7	Run 8	Run 9	Run 10	Run 11	Run 12a	Run 12b
XRD-amorphous	40.3	40.6	30.1	39.3	55.9	56.7	16.1	57.8	52.0	47.2	44.8	23.7	2.4
Goethite												40.6	27.1
Lepidocrocite												8.1	
Magnetite													39.6
Gypsum	55.7	56.9	34.1	47.3	41.9		82.2	38.3	43.2	49.2	53.4	26.0	30.9

oxidised synthetic ARD (containing dominantly Fe^{+3} iron) were treated. Neutralising reagents (see McDonald *et al.* in press, for mineralogical and chemical compositions) were added to the ARD either as a slurry or dry powder (Table 1) and stirred at 450 RPM to ensure good mixing. Once neutralisation was complete, mixing and aeration (if used, Table 1) continued for 18-20 hours. The sludge was allowed to settle for 24 hours, then sludge and treated water were collected for analysis. In Run 1 the sludge was initially greenish in color and then turned brown during air sparging; in Run 2 the sludge was initially green/brown in color and turned brown on oxidation; in Runs 3, 4 and 5 the sludge was initially brown and did not change color. Run 6 used Bauxsol as the neutralising agent, and the sludge retained the red color of this material. In the small batch reactor (Runs 8–11; Table 1), 15 L of the reduced ARD (containing Fe^{+2}iron) was neutralised with a 10 wt% hydrated lime slurry and stirred at 300 RPM to ensure good mixing. The synthetic ARD for all four runs was taken from the same bulk batch to reduce variability. Runs 8 and 9 were air sparged following neutralisation, to promote oxidation of the initially green Fe^{+2} precipitate to a brown Fe^{+3} hydroxide. These runs were duplicates to test variability in the experimental procedure. In Runs 10 and 11, air sparging accompanied neutralisation, and (H_2O_2) was added during neutralisation to further promote the oxidation of Fe^{+2} to Fe^{+3} iron prior to precipitation. Run 11 used a longer dosing period (Table 1) to allow more time for oxidation of the sludge during air sparging. The precipitate in Runs 10 and 11 was initially brown and did not change color. After neutralisation was complete the sludge generated in Runs 8–11 was sparged with compressed air for 18 hours, before being allowed to settle and collected for analysis.

A laboratory scale HDS plant with sludge recycle was used to neutralise oxidised ARD in Run 7; details of the procedure are given in McDonald *et al.* (in press). The sludge formed was brown in color.

Run 12 used a batch analogue of the HDS plant, to allow greater control on the sludge precipitation. Initially 15 L of reduced ARD (without Al) was neutralised with a 10 wt% hydrated lime slurry added using a peristaltic pump and with constant mixing; the sludge was then allowed to settle. The treated water was removed and a 2.5 L batch of reduced, Al-free ARD added and neutralised in the same way; this procedure was repeated for 13 cycles. The sludge was split into two sub-samples; the first (a) was sparged with compressed air continuously until visibly oxidised (~2 days, turning from dark green to light brown), and the second (b) was sparged overnight, allowed to stand for a day (it turned a dark grey/black colour on standing) and then sparged for another 2 days; the colour did not change.

Composition of Sludges
Mineralogical and major element chemical composition of the precipitated sludges was determined by X-Ray Diffraction and X-Ray Fluorescence spectroscopy, respectively. For mineralogical analysis, the proportion of amorphous material was quantified using a ZnO internal standard. If the sludge contained XRD-amorphous material and gypsum, the sample was analysed with a gypsum orientation factor of 0.7-0.8 as recommended by McDonald *et al.* (2005). Trace metals were analysed by Atomic Absorption Spectrometry (AAS) after mixed acid digest method adapted from Eaton *et al.* (1995).

The sludges from all experiments had a high water content (6-40 wt% solids); the weight percent solids was determined from the mass loss on oven drying at 40°C, to ensure that gypsum and other hydrous precipitates were not dehydrated.

The iron component of the sludges varied from amorphous to very finely crystalline; the crystal size is often too small for mineral identification by X-Ray Diffraction. However,

magnetic hysteresis analysis by Vibrating Sample Magnetometry was used to assess the proportion of crystalline material, the crystallite size and also the mineralogy of the iron oxide/hydroxide component, even at nanometer scale (see Appendix for details).

Leach Testing

SALT testing of the sludges from Runs 1–7 (McDonald *et al.* in press) showed little difference in chemical stability. In order to understand the sludge leachability better, the rate of release of metals from sludges during leaching was assessed using a new kinetic test developed during this study.

In this method, 25.0 g of oven-dried (40 °C) ARD treatment sludge was added to a 600 ml beaker along with 500 ml of deionised water, and fully dispersed using sonication for 10 minutes with occasional stirring. The pH was allowed to stabilise for 5 minutes before a slug of concentrated sulphuric acid was added; the volume of H_2SO_4 was not set, but calculated to reduce the solution pH to 4-5. To maintain the pH at 4.0, sufficient 1.4 M H_2SO_4 was added to the stirred sludge using a peristaltic pump to balance the increase in pH due to dissolution of the sludge. 50 ml samples of the stirred sludge and the extractant fluid (leachate) were taken at 5, 15, 30, 45, 60, 90, 120, 180 minutes and 18 hours after the initial dose of H_2SO_4 was added. Each sludge sample was immediately vacuum- filtered to 0.45 μm, acidified and stored for analysis in an airtight container. Filtration took up to 10 minutes in some samples with poor filtering properties. Each sample of leachate was analysed for Cu and Zn by AAS. A mid-range standard was analysed after every 5 samples; if it did not fall within ±5% of the expected value, the instrument was recalibrated and samples reanalysed.

The mass of metal leached (mg) from each sludge sample was calculated by multiplying the measured metal concentration in the leachate for that sample (mg/L) by the volume of water added (0.5 L; volume changes due to acid additions and evaporation were assumed to be insignificant). The mass of metal leached was converted to a percentage of the total metal content of the sludge (previously analysed by AAS after acid digestion).

Results and Discussion

All neutralisations treated the ARD effectively, raising the pH and removing all the dissolved heavy metals (see McDonald *et al.* in press, for treated water compositions from Runs 1–7).

The results of the kinetic leach tests showed substantial differences between the sludges precipitated under oxidising and reducing conditions, and so the results of these runs will be discussed separately. Run 1 was used to develop the analytical methods, and the results are not completely comparable to those from the other runs; therefore it is only briefly discussed below.

Sludge Precipitation from Oxidised ARD (Runs 1–7)

Sludge composition. The sludges from Runs 1–7 consisted predominantly of amorphous ferric oxy-hydroxide and crystalline gypsum (Table 2), other than the Bauxsol sludge (Run 6) which lacked gypsum. In addition, many of the sludges contained a minor calcite phase. The sludges from Runs 1, 3 and 4 (lime and limestone neutralisations) and Run 7 (HDS) have very low values of the magnetic hysteresis parameters ((~3nm) goethite crystallites (see Appendix for explanation). The hysteresis response of sludges from Run 6 (Bauxsol) was very similar to the reagent (**Error! Not a valid bookmark self-reference.**), indicating that the crystallinity of this

sludges is dominated by components inherited from the reagents; this is also evident in the sludge mineralogy (McDonald *et al.* in press).

Rate of Cu and Zn leaching. The leaching of Cu and Zn from the Run 1–7 sludges is initially very rapid and reduces over time, apparently exponentially (Fig. 1 and 2). Approximately 20-30% and 30-40%, respectively of the copper and zinc was leached within the first 5 minutes, representing ~50% of the total amount of these metals leached during the kinetic tests. The rate of release slowed dramatically after 1 hour.

Table 4) indicating that there is very little, if any crystallinity of the iron hydroxide component within these sludges, so they are composed of amorphous ferrihydrite. The sludge from Run 2 and 5 has a higher F/P value and much higher values of M_{rs}/M_s and H_c, indicating the presence of a small component of very fine-grained

Table 3. Chemical composition of ARD Treatment sludge (wt%). See Table 1 for detail on run conditions. (Runs 1-7 after McDonald *et al.* in press)

	Run 1	Run 2	Run 3	Run 4	Run 5	Run 6	Run 7	Run 8	Run 9	Run 10	Run 11	Run 12a	Run 12b
SiO_2[1]	0.09	0.19	0.89	1.02	12.53	13.23	0.05	0.01	0.11	0.08	0.00	0.26	0.11
TiO_2[1]	0	0	0.03	0.03	0.34	4.09	0.01	0.04	0.04	0.04	0.04	0.04	0.04
Al_2O_3[1]	2.62	2.64	1.96	2.65	8.16	14.41	2.47	3.46	3.39	3.16	3.29	0.03	0.04
Fe_2O_3[1]	21.77	21.65	13.31	18.33	18.4	33.07	20.09	31.97	30.84	28.64	30.19	47.04	51.20
MnO[1]	0.04	0.04	0.03	0.04	0.05	0.05	0.04	0.03	0.03	0.02	0.02	0.03	0.04
MgO[1]	0.16	0.12	0.41	0.41	0.68	1.32	0.29	0.09	0.09	0.03	0.04	0.03	0.00
CaO[1]	20.95	19.92	34.03	24.27	17.35	1.38	21.72	17.03	17.86	17.82	15.94	10.80	12.08
Na_2O[1]	0.29	0.28	0.77	0.76	1.00	2.07	1.08	0.93	0.88	0.90	0.87	1.29	1.39
K_2O[1]	0.00	0.00	0.16	0.17	0.27	0.29	0.06	0.00	0.00	0.00	0.00	0.00	0.00
P_2O_5[1]	0.00	0.00	0.02	0.02	0.04	0.11	0.01	0.00	0.00	0.00	0.00	0.02	0.00
SO_3[1]	27.14	28.14	15.74	23.98	20.64	2.17	30.29	20.45	21.04	23.92	22.24	13.43	14.38
CuO^2	1.46	1.46	0.89	1.19	1.17	0.91	1.37	2.02	1.98	1.82	1.96	2.29	2.70
ZnO^2	1.44	1.43	0.87	1.15	1.15	0.89	1.25	1.98	1.92	1.82	1.92	2.90	3.49
LOI^3	24.62	23.95	31.39	26.16	19.02	25.00	22.53	21.92	22.40	22.21	23.21	22.02	14.36
Total	100.53	99.59	100.5	100.18	100.81	98.97	101.25	99.93	100.58	100.46	99.72	100.18	99.83

[1] XRF
[2] Acid Digest then AAS
[3] loss on drying (LOI; 1000°C for 45 minutes).

(~3nm) goethite crystallites (see Appendix for explanation). The hysteresis response of sludges from Run 6 (Bauxsol) was very similar to the reagent (**Error! Not a valid bookmark self-reference.**), indicating that the crystallinity of this sludges is dominated by components inherited from the reagents; this is also evident in the sludge mineralogy (McDonald *et al.* in press).

Rate of Cu and Zn leaching. The leaching of Cu and Zn from the Run 1–7 sludges is initially very rapid and reduces over time, apparently exponentially (Fig. 1 and 2). Approximately 20-30% and 30-40%, respectively of the copper and zinc was leached within the first 5 minutes, representing ~50% of the total amount of these metals leached during the kinetic tests. The rate of release slowed dramatically after 1 hour.

Table 4. Magnetic hysteresis parameters of ARD treatment sludges; Run 6 is dominated by reagent minerals. See Table 1 for details on run conditions. The M_{rs}/M_s ratio reflects the grain size of goethite and/or magnetite crystallites increases, F/P increases with the proportion of goethite and/or magnetite crystallites within the sludge; see Appendix for details. <dl = less than detection limit.

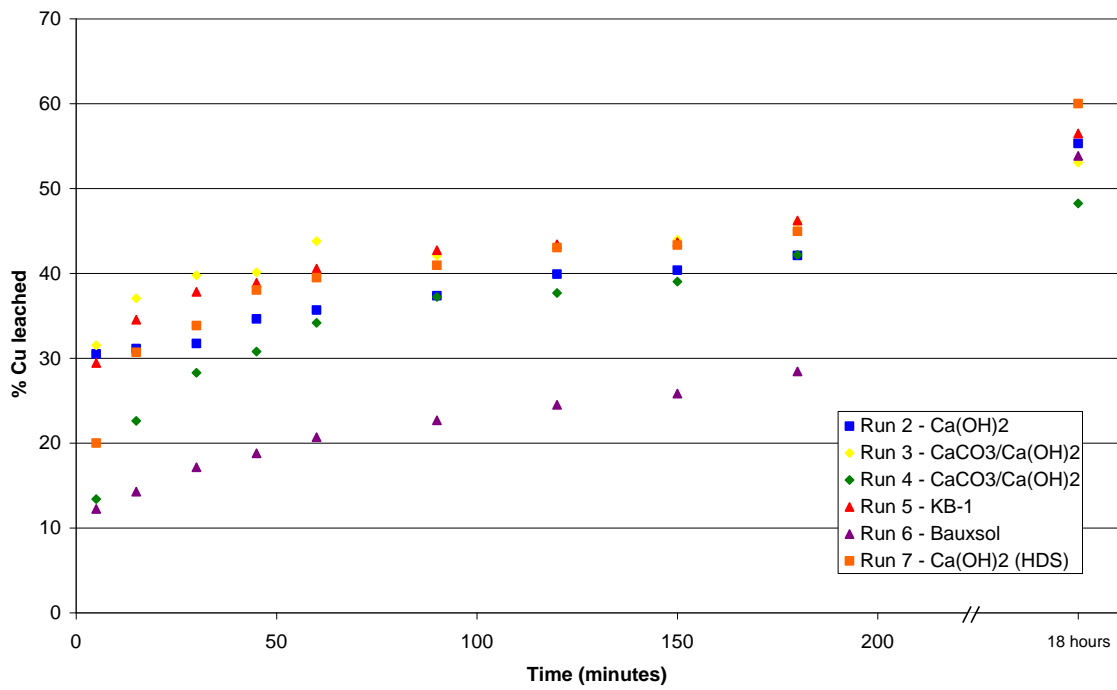| Reagent	Procedure	Reagent used	M_{rs}/M_s	F/P
Bauxsol			0.273	0.8227
	Run 1	$Ca(OH)_2$	<dl	0.0040
	Run 2	$Ca(OH)_2$	0.158	0.0264
	Run 3	$CaCO_3/Ca(OH)_2$	<dl	0.0070
	Run 4	$CaCO_3/Ca(OH)_2$	<dl	0.0047
	Run 5	KB-1	0.078	0.6444
	Run 6	Bauxsol	0.270	0.7095
	Run 7	HDS ($Ca(OH)_2$)	<dl	0.0021
	Run 8	$Ca(OH)_2$	0.025	0.1881
	Run 9	$Ca(OH)_2$	0.036	0.1905
	Run 10	$Ca(OH)_2$	<dl	<dl
	Run 11	$Ca(OH)_2$	<dl	<dl
	Run 12a	$Ca(OH)_2$	0.023	0.2169
	Run 12b	$Ca(OH)_2$	0.116	0.9835

Figure 1. Rate of copper release from sludges precipitated from oxidised ARD
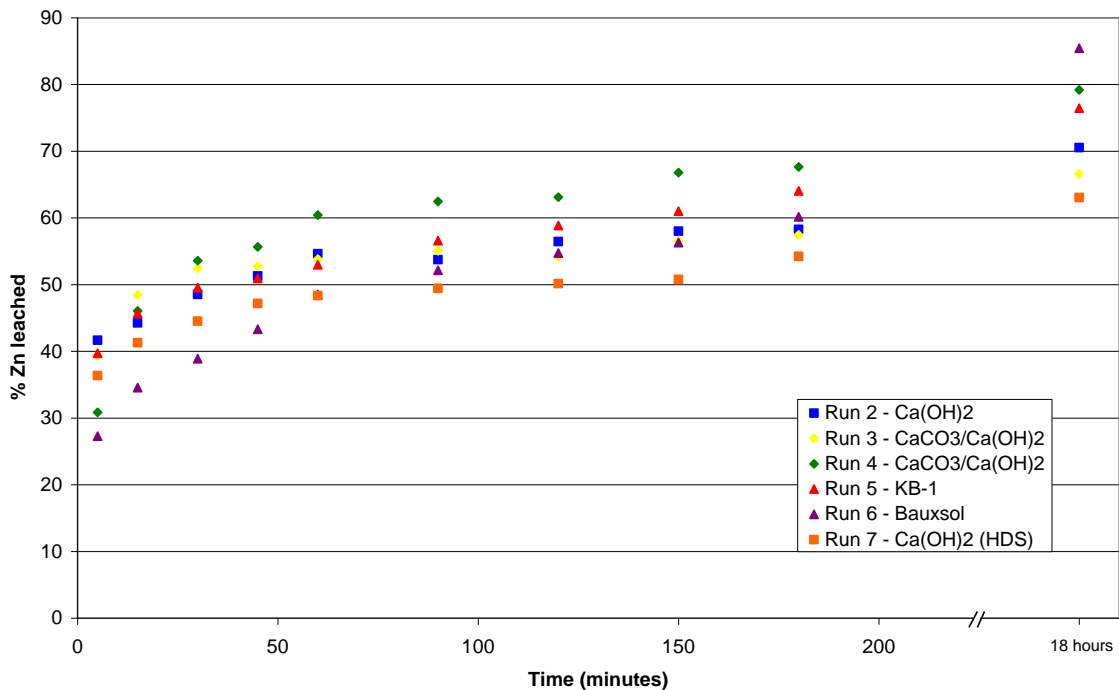

Figure 2. Rate of zinc release from sludges precipitated from oxidised ARD

All the sludges, except that generated from Run 6 (Bauxsol), have similar Cu release curves (Figure 1), and hence exhibit a similar chemical stability with respect to Cu. For Run 6 the

amount of copper leached after 18 hours of mixing was similar to the other runs (Figure 1) but the rate of release was slower; however, the mineral grains within the Bauxsol reagent were too coarse to be suspended by the overhead stirrer used, and thus the slower rate of Cu release may be due to incomplete mixing rather than slower reaction kinetics. Kinetic tests were repeated for Runs 1 and 6 (not shown) to assess reproducibility and variation between repeats was excellent with differences of only 2-4% after 18 hours of mixing. The small variations in the proportion of copper leached from different sludges before 90 minutes are probably not significant. The zinc leach curves (Figure 2) exhibit 10-20% spread in results, consistent with the variations evident in the previous SALT results (McDonald *et al.* in press). Repeat kinetic testing of sludges generated in Runs 1, 2 and 6 (not shown) showed variations of only 3-7% in the amount of zinc leached after 18 hours, indicating that the spread in the proportion of Zn leached over the different runs may be related to slight variations in the neutralisation and leaching procedures rather than the reagent used, because sludges from the two separate limestone neutralisations show ~15% difference in leachability of zinc at the end of the kinetic tests.

After 18 hours all sludges had leached 50-60% of their copper content and 65-85% of their Zn content, and these results compare well with Strong Acid Leach Test (SALT) results from the same sludges (~50% of Cu and 70-90% of Zn leached at pH of 4; McDonald *et al.* in press). Given the variability within the results, there is no difference in chemical stability between sludges formed by standard lime neutralisation and those precipitated by other reagents or processes (KB-1, Run 5; Bauxsol, Run 6; HDS, Run 7). Differences in chemical stability between repeat neutralisations are greater than differences between reagents. These results confirm the previous work of McDonald *et al.* (in press), which showed that Fe, Cu and Zn release from ARD treatment sludges was not dependent on which neutralising reagent/process was used, but on pH. Hence a sludge's chemical stability is governed by its neutralising potential, because sludges with a higher neutralisation potential can neutralise a larger volume of acid before the pH drops to levels where the metals in the sludge are mobilised.

The initial rapid release of large amounts of Cu and Zn from all sludges, over a period of minutes, shows that ARD neutralisation sludges will quickly leach adsorbed metals into acid water. This is potentially of great concern, as it indicates that if the sludges are placed in an acid environment, even for a short time, they will rapidly liberate substantial amounts of heavy metals into the surrounding ground or surface waters.

Copper and Zn are probably present in ARD treatment sludges as hydroxide species adsorbed onto the surface of the poorly crystalline Fe^{+3} oxyhydroxide (Kinniburgh *et al.* 1976, Webster *et al.* 1998), and desorbtion of these metal species occurs under low pH conditions. The initial very rapid release of Cu and Zn during the kinetic tests followed by the exponentially decreasing rate of metal release with time (Fig. 1 and 2) is probably indicative of surface desorption reactions tending towards equilibrium.

Sludge Precipitation from Reduced ARD (Runs 8–11)

To determine whether the oxidation state of iron during ARD neutralisation affected the chemical stability of the sludges precipitated, the synthetic ARD composition used in Runs 8–11 contained only reduced iron (as Fe^{+2}). Given that the results of Runs 1–7 showed that the neutralisation reagent had no effect on sludge leachability, in Runs 8–11 only $Ca(OH)_2$ was used for neutralisation. During Runs 8 and 9 the sludge precipitated as a green (ferrous) material and turned brown as it was oxidised with air sparging; in Runs 10 and 11 a brown (ferric) precipitate formed.

<u>Sludge composition.</u> The brown sludges formed in Runs 10 and 11 have the same color as those formed by lime neutralisation in Runs 1 and 2, whilst the sludges formed in Runs 8 and 9 are slightly darker. The sludges from Runs 8–11 have a similar mineralogical and chemical composition to each other, consisting mainly of amorphous Fe^{+3} oxy-hydroxide (ferrihydrite) and crystalline gypsum (Tables 2 & 3). However, the magnetic hysteresis analyses for the Run 8 and 9 sludges (precipitated as Fe^{+2} iron and then oxidised) show that they have much higher values of the M_{rs}/M_s and F/P ratios than the sludges initially precipitated as oxidised $Fe(OH)_3$ (Runs 10 and 11; (~3nm) goethite crystallites (see Appendix for explanation). The hysteresis response of sludges from Run 6 (Bauxsol) was very similar to the reagent (**Error! Not a valid bookmark self-reference.**), indicating that the crystallinity of this sludges is dominated by components inherited from the reagents; this is also evident in the sludge mineralogy (McDonald *et al.* in press).

<u>Rate of Cu and Zn leaching.</u> The leaching of Cu and Zn from the Run 1–7 sludges is initially very rapid and reduces over time, apparently exponentially (Fig. 1 and 2). Approximately 20-30% and 30-40%, respectively of the copper and zinc was leached within the first 5 minutes, representing ~50% of the total amount of these metals leached during the kinetic tests. The rate of release slowed dramatically after 1 hour.

Table 4). Thus, the Run 8–9 sludges contain very fine-grained goethite crystallites, whereas the Run 10–11 sludges are composed entirely of amorphous ferrihydrite. The goethite crystallites are likely to be less than 20 Å in size as they were not detected by XRD (Jenkins and Snyder 1996).

<u>Rate of Cu and Zn leaching.</u> The initial release of Cu and Zn from the Run 8 and 9 sludges during the kinetic leach tests is much less than from the Run 10 and 11 sludges and is also less than from the Run 1–7 sludges (Fig. 3 and 4). Less than 5% of the Cu was released from Run 8 and 9 sludges in the first 5 minutes (Figure 3), compared to 15-25% for Run 10 and 11 sludges and 15-30% for Run 1–7 sludges (Figure 1). However, after 180 minutes the differences are less marked, with the amounts of Cu leached being 19-29%, 36-39% and 45%, respectively, and after 18 hours the proportion of Cu released from Run 8 and 9 sludges is only 5-10% less than that leached in the other kinetic tests (Figure 3). Zinc leaching shows similar trends (Figure 4), with the proportion of Zn released from Run 8 and 9 sludges being significantly lower than from other sludges prior to 180 minutes in the kinetic tests, but only 5-10% less after 18 hours.

These results show that ARD neutralisation sludge precipitated as $Fe(OH)_2$ and then oxidised to Fe^{+3} oxyhydroxide (Runs 8 and 9) has a much slower rate of Cu and Zn release than sludge precipitated directly as $Fe(OH)_3$ (Runs 10 and 11). The difference reflects the iron mineralogy of the sludges as revealed by the magnetic hysteresis parameters; the Run 8 and 9 sludges contain goethite crystallites absent in the Run 10 and 11 sludges. It seems probable that the Cu and Zn are incorporated into the goethite crystal structure rather than adsorbed onto the surface of the goethite crystallites, because the rate of metal loss during the first 5 minutes of the kinetic testing is relatively slow, compared to the much more rapid initial loss of surface-adsorbed Cu and Zn from the ferrihydrite sludges (Fig. 3 and 4). Goethite can contain 5 and 11 mole% of Cu and Zn, respectively, substituted for Fe (Cornell and Schwertmann 2003, Gerth *et al.* 1985).

At least some of the Al content of the Run 8 and 9 sludges (Table 3) is probably incorporated into the goethite. Al can substitute for Fe in goethite up to 32 mole% (Fitzpatrick and Schwertmann 1982), and causes a reduction in unit cell dimension (Schulze 1984), because Al is 17% smaller than Fe. The presence of Al in the Run 8–9 goethite cannot be verified because the crystallites are too small for the decrease in unit cell size to be detected by XRD. Structural Al within goethite reduces its dissolution rate in strong acids (Schwertmann 1984, Torrent *et al.* 1987), and helps to explain the slow rate of copper and zinc release from the Run 8-9 sludges.

By the end of the kinetic tests (after 18 hours) the percentage of metals leached is only slightly less in the Run 8 and 9 sludges than in the sludges lacking goethite (Runs 10 & 11). Perhaps the tiny goethite crystallites cannot withstand prolonged acid attack; particle size of iron oxides has a marked effect on crystallite solubility (Cornell and Schwertmann 2003). Nevertheless it is clear that sludges precipitated as ferrous oxyhydroxide and then oxidised to ferric oxyhydroxide are more chemically stable under acid leaching and release less Cu and Zn than sludges initially precipitated as $Fe(OH)_3$.
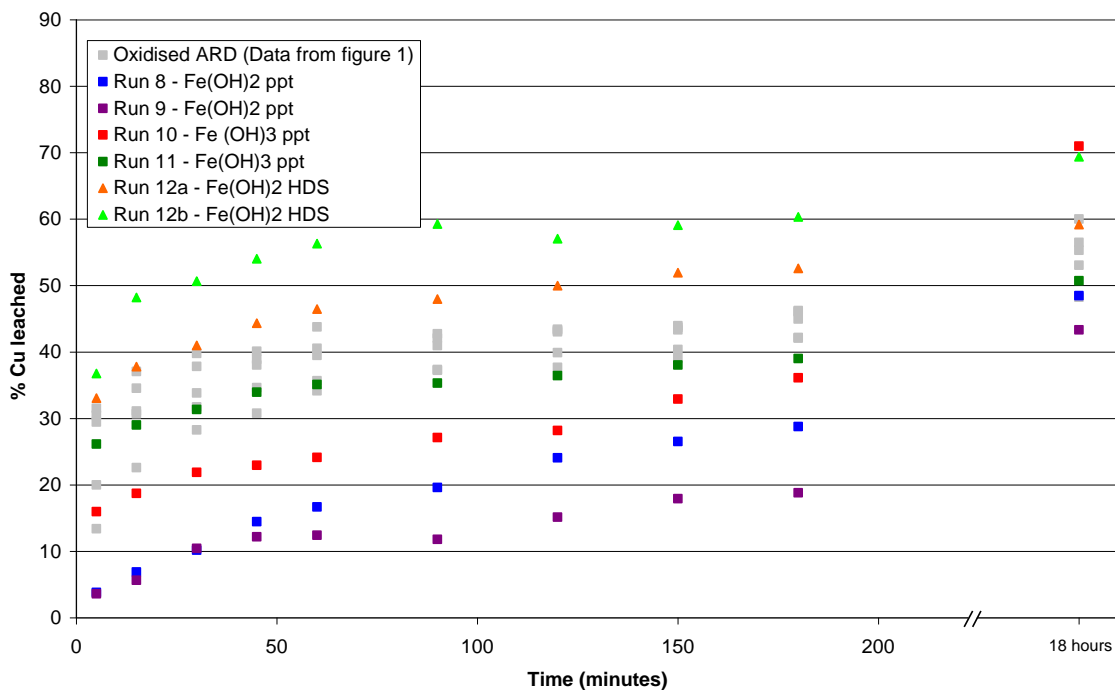

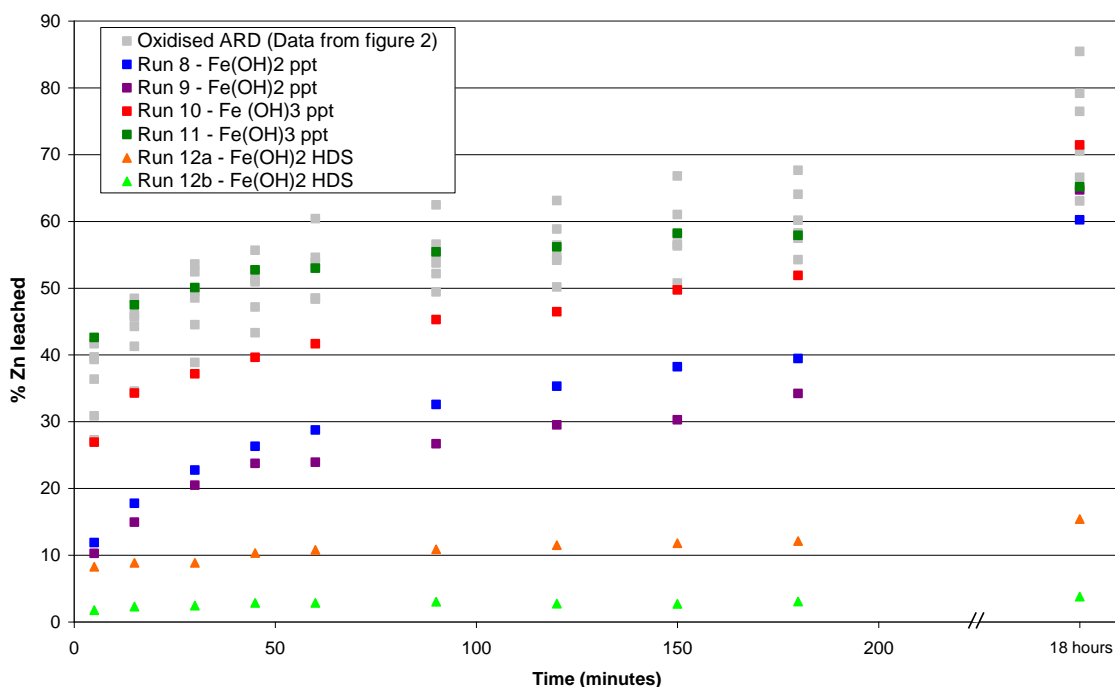Figure 3. Rate of copper release from sludges precipitated from reduced ARD

Figure 4. Rate of zinc release from sludges precipitated from reduced ARD

Sludge Precipitation from Al-free Reduced ARD (Run 12)

The results of Runs 8 and 9 indicated that sludges with increased crystallinity have greater resistance to acid leaching. In order to increase the sludge crystallinity, in Run 12 Al was omitted from the synthetic ARD because it inhibits the crystal growth of iron oxides and hydroxides (Cornell and Schwertmann 2003). In addition, the Al-free reduced ARD was neutralised using a batch analogue to the HDS process, in the hope that this procedure would allow the initial crystallites to act as seed crystals in the recycle process and increase the crystal size within the sludge.

Sludge composition. The sludge generated in Run 12 was split into two subsamples; the first (a) was sparged with compressed air continuously until completely oxidised, turning from dark green to light brown, and the second (b) was sparged overnight, allowed to stand for a day and then sparged for another 2 days, turning a dark grey – black color. Whilst the two sludges are chemically similar (Table 3), they differ substantially in color and mineralogy (Tables 2 & 4). The brown Run 12a sludge contains goethite, minor lepidocrocite, and a substantial component of XRD-amorphous $Fe(OH)_3$ (29.7 wt%), and a high value of the magnetic parameter F/P, indicating a large proportion of iron oxide/hydroxide crystallites within the sludge. In contrast, the dark grey – black Run 12b sludge contains magnetite, goethite and only 2.4 wt% XRD-amorphous $Fe(OH)_3$, and has high M_{rs}/M_s and F/P values due to the presence of abundant, relatively coarse-grained iron oxide/hydroxide crystallites within the sludge. The proportion of XRD-amorphous $Fe(OH)_3$ in the Run 12a and 12b sludges is much less than in almost all the other sludges (Table 2) because much of the iron is present as crystalline phases. The much lower structural water content of the Run 12b sludge (LOI, Table 3) reflects its substantial content of non-hydrated iron oxide (magnetite).

The presence of magnetite in the Run 12b but not Run 12a sludge is presumably due to the fact that the Run 12b sludge was partially oxidised, allowed to stand and then fully oxidised. Magnetite ($Fe^{+2}Fe^{+3}_2O_4$) contains both Fe^{+2} and Fe^{+3} iron, and so cannot form from a Fe^{+3} solution or precursor under fully oxidising conditions. Magnetite precipitation by oxidative hydrolysis of Fe^{+2} salts is also pH controlled, and requires a pH of over 8 (Schwertmann and Cornell 2000).

The greater crystallinity of the Run 12 sludges and the presence of magnetite is almost certainly due to the lack of Al in the ARD; Al inhibits the crystal growth of iron oxides and hydroxides (Cornell and Schwertmann 2003), and suppresses the formation of magnetite in preference to goethite (Schwertmann and Murad 1990). For this reason most ARD neutralisation sludges formed during mine site treatment lack crystalline iron oxide/hydroxide minerals; a rare exception is the lepidocrocite present in sludge from the Geco HDS plant in Canada (Aube and Zinck 1999), where the ARD contained 600 mg/L Fe and only 10 mg/L Al.

Rate of Cu and Zn leaching. The amount of Cu leached from Run 12a and 12b sludges was slightly greater than for all other sludges, and the rate of release over the first 5 minutes of the kinetic testing was much more rapid (Figure 3). In contrast, Zn release was about an order of magnitude lower than for the other sludges, and considerably slower (Figure 4). At the end of the kinetic tests, 60-70% of the Cu but only 5-15% of the Zn had been leached from the Run 12 sludges, compared to 50-60% and 60-80%, respectively for all other sludges. The brown goethite-rich Run 12a sludge released more Zn and less Cu than the grey/black magnetite-goethite Run 12b sludge, and the difference between them (~10%) is greater than the experimental variability of the results for Runs 1, 2 & 6 (2-7%, as discussed previously).

The leach results reflect the greater crystallinity of these sludges (Tables 2 & 4). Zinc is most probably incorporated into the crystal structure of both the goethite and magnetite within the sludge, making it less susceptible to acid leaching. As previously discussed, goethite can incorporate up to 11 mole% Zn, and magnetite can contain as much as 17% Zn randomly distributed within the crystal structure replacing octahedral Fe^{+2} (Sidhu *et al.* 1978, Sidhu *et al.* 1981). The greater resistance of the Run 12 sludges to acid leaching of their Zn contents is due to the much more abundant crystallites within these sludges. The Run 8 and 9 sludges, which contain a smaller proportion of probably finer-grained goethite, release Zn more readily (Figure 4).

The Cu within the Run 12 sludges is almost certainly adsorbed to the surfaces of the goethite and magnetite crystallites, and is therefore quickly released as soon as the surfaces are exposed to acid leaching (Fig. 3). Sidhu *et al.* (1978) found that Cu in synthetic magnetites was concentrated near the surface of the crystals, as shown by an initial very rapid release of Cu during acid dissolution. Interestingly, the kinetic testing of the Run 8 and 9 sludges indicated that they contain goethite with copper incorporated into the crystal structure, yet the Run 12 sludges show no evidence of this. The difference may reflect the much higher Al content of the Run 8 and 9 sludges (Table 3); at least some of this Al is likely to be incorporated into the goethite structure, as previously mentioned. Because Al is smaller than Fe, substitution of Al in goethite reduces the unit cell dimension (Schulze 1984) and this may make it easier for Cu to be incorporated into the goethite lattice. Thus, the enhanced Cu mobility of the Run 12 sludges may be due to the lack of Al within these sludges.

Conclusions - Implications for leachability of ARD neutralisation sludges

The kinetic tests have shown that in sludges formed by standard ARD neutralisation procedures and reagents (lime, limestone, Bauxsol, KB-1 and HDS lime), heavy metals like Cu and Zn are adsorbed onto the surface of the amorphous ferrihydrite, and are very rapidly released if the sludge is exposed to acid conditions. The sludges formed by the different reagents and procedures all exhibit much the same chemical stability; this was also shown by McDonald *et al.* (in press) using the Strong Acid Leach Test. Therefore, it is important to ensure that ARD treatment sludges do not come into contact with acid waters, even for short periods of time. Sludges with a high neutralising potential are more resistant to acid leaching only in the sense that they can neutralise more acid in pore waters before the pH reduces to levels where heavy metal leaching occurs.

However, if the sludge contains a crystalline iron oxide/hydroxide component (goethite/ lepidocrocite/magnetite), the Zn leachability dramatically decreases, by almost an order of magnitude, both in terms of the rate and total amount of zinc released, due to the incorporation of Zn within the mineral structure. This is particularly marked if the iron oxide/hydroxide minerals are relatively coarse-grained (detectable by XRD). Therefore the precipitation of at least partly crystalline sludges potentially offers considerable advantages in chemical stability and resistance to acid leaching. Control of redox conditions during neutralisation and the Al concentration of the ARD are crucial in this regard.

Increasing the crystalline iron oxide/hydroxide content of an ARD treatment sludge has a mixed effect on the leachability of copper. This metal is more readily released from sludges with a higher goethite/magnetite content precipitated from Al-free ARD, because the Cu has been excluded from the structure of these minerals and is adsorbed on the crystallite surfaces. However, it appears that Al-rich goethite can incorporate Cu, reducing its leachability. Further work is needed for a detailed understanding of the controls on Cu release, but nevertheless crystalline sludges offer benefits by either increasing the resistance to Cu leaching, or removing Cu in a form that can be easily released at a later stage under controlled conditions.

The production of crystalline sludges has an added benefit in that the crystalline iron oxide/hydroxide minerals (particularly magnetite) have a greater density and lower water content than ferrihydrite, therefore increasing the bulk density of the sludge and reducing the volume required for storage. Furthermore, if magnetite is the main iron mineral in the precipitate, it can be simply magnetically separated from the other component of the sludge, usually gypsum, giving two potentially marketable waste streams. This could provide income and at the same time do away with the problem of sludge disposal.

Therefore modifications to the method of neutralisation during ARD treatment, particularly control of Al content and oxidation state, offer the potential to substantially improve the chemical stability of the sludge precipitated, and have a much greater influence than the neutralisation agent used. These modifications could also lead to the production of saleable treatment products and large savings to water treatment plant operators. If the benefits are realised, these modification are likely to become a fundamental part of ARD active treatment systems, and are probably applicable to any water treatment sludges formed by pH adjustment, e.g. pickle liquor industry, metal plating, landfill leachate, as well as acid rock drainage.

Acknowledgements

References

Aube, B. C. and Zinck, J. M. 1999. Comparison of AMD treatment processes and their impact on sludge characteristics. p. 261-270. *In* Goldsack, D.; Belzile, N.; Yearwood, P. and Hall, G. (eds.) Sudbury '99; Mining and the environment II. (Sudbury, Ontario, Canada, 13-17 September 1999).

Brown, M.; Barley, B. and Wood, H. 2002. Minewater treatment: technology, application and policy. pp. 453. IWA Publishing: London.

Cornell, R. M. and Schwertmann, U. 2003. The iron oxides: structure, properties, reactions, occurences and uses. 2nd ed., pp. xxxix, 664. Wiley-VCH: Weinheim; [Cambridge]. http://dx.doi.org/10.1002/3527602097.

Earth Systems. 2004. Process design for active treatment of ARD at the Brukunga mine site. July 2004.

Eaton, A. D.; Clesceri, L. S. and Greenberg, A. E., (Eds.) 1995. Standard methods for the examination of water and wastewater. 19th ed. APHS-AWWA-WEF: Washington, D.C.

Fitzpatrick, R. W. and Schwertmann, U. 1982. Al-substituted goethite; an indicator of pedogenic and other weathering environments in South Africa. Geoderma 27 (4); 335-347. http://dx.doi.org/10.1016/0016-7061(82)90022-2.

Gerth, J.; Davey, G. B. and Cockayne, D. J. H. 1985. Incorporation of trace metals and radionuclides into goethite. p. 108-110. *In* 4th Austalian Conference on Nuclear Techniques of Analysis. 6-8 November 1985) Australian Institute of Nuclear Science and Engineering (AINSE).

Jenkins, R. and Snyder, R. L. 1996. Introduction to X-ray powder diffractometry. Chemical analysis; v. 138., pp. xxiii, 403. Wiley: New York.

Kinniburgh, D. G.; Jackson, M. L. and Syers, J. K. 1976. Adsorption of alkaline earth, transition, and heavy metal cations by hydrous oxide gels of iron and aluminum. Soil Science Society of America Journal 40 (5); 796-799 http://dx.doi.org/10.2136/sssaj1976.03615995004000050047x.

Kuyucak, N.; Mattsson, E. and Bringsaas, H. 2005. Implementation of a site-specific high density sludge process for treating high strength acid mine drainage at the Falu Mine Site, Falun, Sweden. p. 546-555. *In* Securing the Future: international conference on mining and the environment, metals and energy recovery. (Skelleftea, Sweden, 27 June - 1 July 2005).

Lewis, M. N.; Wangerud, K. W.; Park, B. T.; Rundingsland, S. D. and Jonas, J. P. 2003. Status of in-situ treatment of Anchor Hill pit lake, Guilt Edge mine superfund site, South Dakota,

USA. p. 779-788. *In* Sixth international conference on acid rock drainage. (Cairns, Australia, 14-17 July 2003).

McDonald, D.; Webb, J.; Ruddick, M.; Woollard, J. and Glaisher, R. 2005. Quantifying the amorphous content of acid rock drainage (ARD) treatment sludge using XRD and XRF. p. 111. *In* Australian X-ray Analytical Association 2005 Schools and Conference. (Fremantle, Western Australia, 14-18 February 2005).

McDonald, D.; Webb, J. and Taylor, J. in press. Chemical stability of acid rock drainage treatment sludge and implications for sludge management. *Environmental Science & Technology*.

Portefield, D. C.; Miller, S. and Waters, P. 2003. A Strategy for managing acid rock drainage in arid climates – The Mt Whaleback story. p. 143-146. *In* Sixth international conference on acid rock drainage. (Cairns, Australia, 14-17 July 2003).

Schulze, D. G. 1984. The influence of aluminum on iron oxides; VII, Unit-cell dimensions of Al-substituted goethites and estimation of Al from them. Clays and Clay Minerals 32 (1); 36-44. http://dx.doi.org/10.1346/CCMN.1984.0320105.

Schwertmann, U. 1984. The influence of aluminium on iron oxides; IX, Dissolution of Al-goethites in 6M HCl. Clay Minerals 19 (1); 9-19. http://dx.doi.org/10.1180/claymin.1984.019.1.02.

S Schwertmann, U. and Murad, E. 1990. The influence of aluminum on iron oxides; XIV, Al-substituted magnetite synthesized at ambient temperatures. Clays and Clay Minerals 38 (2); 196-202. http://dx.doi.org/10.1346/CCMN.1990.0380211.

Schwertmann, U. and Cornell, R. M. 2000. Iron oxides in the laboratory: preparation and characterization. 2nd ed., pp. xiv, 137. Vch: Weinheim; New York. http://dx.doi.org/10.1002/9783527613229.

Sidhu, P. S.; Gilkes, R. J. and Poser, A. M. 1978. The synthesis and some properties of Co, Ni, Zn, Cu, Mn, and Cr substituted magnetites. *Journal of Inorganic and Nuclear Chemistry **39***; 1953-1958.

Sidhu, P. S.; Gilkes, R. J. and Poser, A. M. 1978. The synthesis and some properties of Co, Ni, Zn, Cu, Mn, and Cr substituted magnetites. Journal of Inorganic and Nuclear Chemistry 39; 1953-1958. http://dx.doi.org/10.1016/0022-1902(77)80523-X.

Stumm, W. and Morgan, J. J. 1996. Aquatic chemistry: chemical equilibria and rates in natural waters. 3rd ed.; Environmental science and technology., pp. xvi, 1022. Wiley-Interscience: New York.

Torrent, J.; Schwertmann, U. and Barron, V. 1987. The reductive dissolution of synthetic goethite and hematite in dithionite. Clay Minerals 22 (3); 329-337. http://dx.doi.org/10.1180/claymin.1987.022.3.07.

Watzalf, G. R. and Casson, L. W. 1990. Chemical Stability of Manganese and Iron in Mine Drainage Treatment Sludge. p. 3-9. *In* Mining and Reclamation Conference and Exhibition. (Charleston, West Virginia, 23-26 April 1990) West Virginia University.
https://doi.org/10.21000/JASMR90010003

Webster, J. G.; Swedlund, P. J. and Webster, K. S. 1998. Trace metal adsorption onto an acid mine drainage iron(III) oxy hydroxy sulphate. Environmental Science & Technology 32 (10); 1361-1368. http://dx.doi.org/10.1021/es9704390.

Appendix: Determination of the crystallinity and mineralogy of ARD neutralisation sludges using magnetic hysteresis

ARD neutralisation sludges are generally amorphous to extremely finely crystalline; the crystal size is often too small for mineral identification by X-Ray Diffraction. However, measurement of magnetic hysteresis parameters on a vibrating sample magnetometer (VSM) can determine the proportion of crystalline material and the crystallite size of the iron oxide/hydroxide minerals present; e.g. ultrafine nanodots of goethite with diameters averaging 3.5 nm have been identified by their magnetic properties (Guyodo *et al.* 2003).

In the magnetic hysteresis procedure the magnetisation response (M) of a vibrating sample is measured during a cycle in which an applied magnetic field (H) is raised from zero to 1 Tesla and reduced back to zero, then increased in the opposite direction and returned to zero. Paramagnetic materials (e.g. ferrihydrite) exhibit a linear hysteresis relationship between the applied field (H) and the magnetisation (M). Ferromagnetic materials (both ferrimagnets, e.g. magnetite and antiferromagnets, e.g. goethite) produce a non-linear hysteresis response, such that the forward M-H path (where H is growing) is different to that of the reverse path (where H is decreasing). The width and shape of the gap between the forward and reverse paths reflect the energy required to change the magnetisation direction of the material. By examining the hysteresis path at high H, where the ferromagnetic minerals are saturated, the contribution of the paramagnetic minerals can be identified and subtracted, to leave a hysteresis path for the ferromagnetic component alone.

In ferrimagnetic minerals, magnetisation energy increases as grains grow from nanometre to micrometre size, passing from a superparamagnetic state to a condition in which grains contain a stable single magnetic domain. The scale at which this occurs depends on mineralogy and grain shape, but in magnetite it is typically 100 nm to 1 μm. Further growth results in the formation of multiple domains in a single grain, lowering the magnetisation energy. Antiferromagnetic minerals (e.g. goethite) in general support much lower magnetisations than do ferrimagnetic minerals, owing to near perfect cancellation between their two antiparallel magnetic sublattice sets. However, ultrafine goethite, in the form of nanodots with diameters averaging 3.5 nm, has been reported to exhibit ferrimagnet-like properties (Guyodo *et al*. 2003), presumably because such small grain size results in increased proportions of grains with an odd number of sublattices, causing incomplete cancellation.

In poorly crystalline iron oxide/hydroxide ARD neutralisation sludges, initial nucleation of crystallites will be revealed in a shift from the paramagnetic behaviour of ferrihydrite to a ferromagnetic hysteresis loop; early growth stages should see an increase in the magnetisation energy as shown by the width and "squareness" of the loop. In samples where the antiferromagnetic mineral goethite is nucleating, the magnetisation energy should increase until the first-formed nanodots begin to aggregate to form nanorods, typically with lengths > 10 nm, and will then rapidly decrease. Samples with antiferromagnet (magnetite) crystallites should have wider hysteresis loops than samples with ferrimagnet crystallites of comparable size.

The nucleation and growth of iron oxide/hydroxide crystallites within ARD neutralisation sludges can be assessed using several parameters derived from the hysteresis loops. Firstly, the paramagnetic contribution due to ferrihydrite can be determined by the slope of the magnetisation response (M) to the applied magnetic field (H) at high values of H (> 800 mT; Fig. A1); this slope is then subtracted from the entire hysteresis path, to leave a loop due to

ferromagnets alone (Fig. A2). Then the saturation magnetisation (M_s), net magnetisation at 1000 mT (M_{1000}), saturation remanence (M_{rs}) and coercivity (H_c) can be measured from the ferromagnet hysteresis loop (Fig. A2). The extent of ferromagnet crystallite formation is indicated by the ratio M_s/M_{1000}, which is here termed F/P (ferromagnets/paramagnets); higher values of the ratio indicate a higher percentage of crystallites of goethite and/or magnetite, although this is complicated to a minor extent by grain size and mineralogy (Fig. A3). If the concentration of ferromagnetic grains is constant, the F/P ratio is higher for magnetite than goethite, and reaches a maximum for goethite at a grain size of ~10nm and for magnetite at a grain size of 100-1000nm; at coarser grain sizes the F/P ratio decreases. The "squareness" of the hysteresis loop, given by M_{rs}/M_s, measures the magnetisation energy; values of this ratio will generally rise as the grain size of ferromagnetic (goethite and magnetite) crystallites increases. However, as goethite crystallises, in the very earliest stages of nucleation (nanodots, too small to register using XRD analysis), the M_{rs}/M_s ratio suddenly jumps, followed by a rapid decrease as the average grain size increases (as nanodots aggregate to nanorods; Fig. A3). The M_{rs}/M_s ratio is independent of the concentration of ferromagnetic grains, so samples with very low levels of nucleation will have a finite M_{rs}/M_s value although it may be undetectable unless very sensitive equipment is used. The M_{rs}/M_s ratio for antiferromagnetic minerals like goethite increases rapidly to a maximum at a grain size of ~3-10 nm, then decreases to very low values as grain size increases further. Ferrimagnetic minerals like magnetite show a more gradual increase in M_{rs}/M_s to a maximum at a grain size of around 50-100 nm, followed by a slow decrease; the highest M_{rs}/M_s value for magnetite is less than that for goethite (Fig. A3).
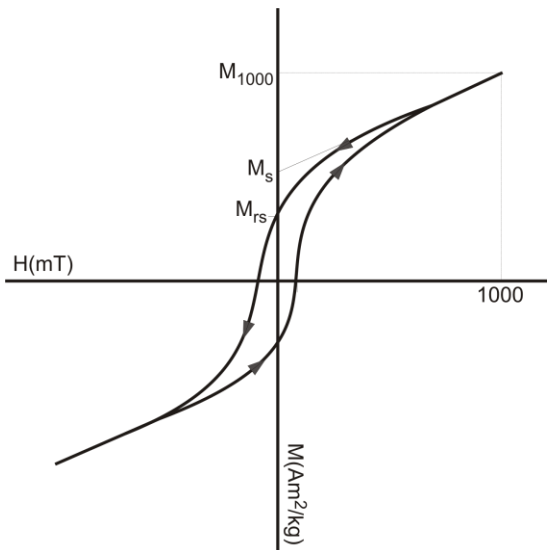

Figure A1. Typical magnetic hysteresis loop for a mixture of ferro- and para-magnetic minerals.
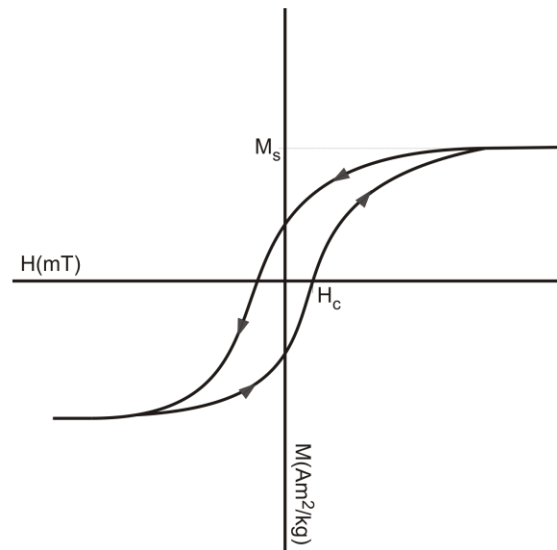
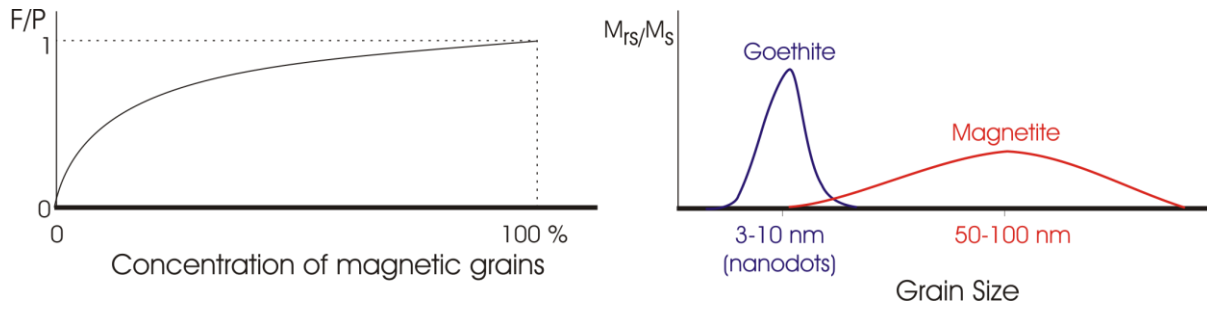Figure A2. Typical magnetic hysteresis loop for a ferromagnetic mineral.

Figure A3. Response of magnetic properties M_{rs}/M_s and F/P to grain size and concentration of magnetic grains. Note that M_{rs}/M_s is independent of the concentration of magnetic grains, and F/P is controlled to a minor extent by grain size.

Guyodo, Y., Mostrom, A., Penn, R.L., and Banerjee, S.K., 2003. From Nanodots to Nanorods: Oriented aggregation and magnetic evolution of nanocrystalline goethite. *Geophysical Research Letters*, **30**, 1512.